Probabilistic Engineering Mechanics 53 (2018) 66–74

Contents lists available at ScienceDirect

Probabilistic Engineering Mechanics

journal homepage: www.elsevier.com/locate/probengmech

Multiple timescale spectral analysis of a linear fractional viscoelastic system under colored excitation

V. Denoël

Structural Engineering Division, Faculty of Applied Sciences, University of Liège, Liège, Belgium

ARTICLE INFO

Keywords:
Caputo fractional derivative
Riemann–Liouville fractional derivative
Perturbation analysis
Stochastic averaging
Background component
Resonant component

ABSTRACT

This paper specifies the multiple timescale spectral analysis to the structural analysis of a single degree-of-freedom structure including a fractional derivative constitutive term. Unlike usual existing models for this kind of structure, the excitation is also assumed to be colored, in a low-frequency range compared to that of the structural system, but not necessarily as an integer autoregressive filter. This problem further extends the domain of applicability of the multiple timescale spectral analysis. The solution is developed as a sum of background and resonant components. Because of the specific shape of the frequency response function of a system equipped with a fractional viscoelastic device, the background component is not simply obtained as the variance of the loading divided by the stiffness of the system. On the contrary the resonant component is expressed as a simple extension of the existing formulation for a viscous system, at least at leading order. As a validation case, the proposed solution is shown to recover similar results (in the white noise excitation case) as former studies based on a stochastic averaging approach. A better accuracy is however obtained in case of very small fractional exponent. Another example related to the buffeting analysis of a linear fractional viscoelastic system demonstrates the accuracy of the proposed formulation for colored excitation. This paper is mostly illustrated with the structural analysis of systems equipped with fractional dampers, but it could be re-interpreted in any of the many other fields of engineering where applications are governed by the same equation.

1. Introduction

Fractional calculus has attracted considerable attention over the last decades, partly due to the versatility of fractional-order tools to model biological [1,2], biomedical [3], financial [3] as well as mechanical and structural engineering applications. In mechanics, fractional derivatives are used to model viscoelastic devices [4], whose properties are extracted from dedicated experimental procedures [5]. The stochastic dynamic analysis of systems with fractional viscoelastic devices has been extensively covered, from linear to nonlinear systems and in various cases of stationarity and Gaussianity limitations, and with various type of loadings.

The linearity of the Riemann–Liouville operator [6] makes it rather straightforward to combine viscoelastic devices with others existing features of stochastic dynamics, like frequency dependent parameters [7] or linear systems control theory [8]. It makes it also rather straightforward to generalize the convolution integral [9,10] or the augmented state formulation [11] to that class of problems. The nonstationary solution of linear systems might also be expressed in closed form [12]. As soon as nonlinear stochastic dynamical systems are considered, the exact solution is usually not obtained in closed form, even for wide-band (usually white noise) excitation. Approximations similar to or derived from the stochastic linearization and stochastic averaging methods [13–16], or those based on a Fokker–Planck equation of the process envelope [17] appear to be the most classical ways to deal with such problems. Narrow band excitations and complex dynamical interactions can be simplified with similar multiple scales approaches [18]. Other more realistic types of loadings [19] or even earthquake loadings of linear and nonlinear systems equipped with viscoelastic devices have been considered [20,21].

Beside these approximations of the exact solution of the problem, other numerical techniques have been proposed to deal with the structural analysis of systems with fractional derivatives. In particular, Monte Carlo simulation methods are consistently used to validate approximations. There exist also *ad hoc* simulation methods [12,22] which are computationally efficient, methods based on Wiener path integral approaches [23–26] and weak formulations based on wavelet transforms [27]. These techniques, together with exact assembling procedures of structural analysis [28], or finite element approaches [29–31], make it possible to study more realistic structures composed of several beams and columns, and several viscoelastic devices.

E-mail address: v.denoel@uliege.be.

https://doi.org/10.1016/j.probengmech.2018.05.003
Received 25 December 2017; Received in revised form 1 April 2018; Accepted 8 May 2018

This review of the literature reveals two trends. On one side, there are simple dynamical systems with linear (or linearized) behavior and white noise excitation, which possess closed form solutions. On the other side, there are numerical techniques to deal with more realistic loadings (sometimes nonstationary), more realistic structures and/or slight nonlinearities. The missing gap in-between is related to the understanding (via simple analytical solutions) of the behavior of complex structures subjected to more realistic loadings. As a first step towards this goal, we consider the stochastic analysis of a linear system subjected to a low frequency loading specified by its arbitrary power spectral density. This problem could be studied by means of the usual time domain multiple scales approach, or the stochastic averaging approach, but would require the consideration of three interacting timescales as well as fractional models —similar to those used to simulate realizations of wind fields [32]—for the augmented state coloring the excitation. This seems possible to solve the problem in this way, although no track evidences of this type of problem has been found in the literature. Instead, we take advantage of the linearity of the problem to derive a simplified solution in a frequency domain. It is based on the Multiple Timescale Spectral Analysis [33] which seeks the same objectives as the stochastic averaging, with slightly more versatility. This method has already been applied in the context of non Gaussian loading [34], nonstationary loading [35] slightly nonlinear systems [36] or multi degree-of-freedom structures [37,38]. The problem considered in this paper is just a little extension of the method and further studies could combine viscoelastic devices with slight nonlinearities or multiple degrees-of-freedom, for instance.

2. Problem formulation

The governing equation of motion of a linear single-degree-of-freedom system equipped with a viscoelastic device reads

$$m\ddot{y}(t) + gD^{\alpha}y(t) + ky(t) = f(t) \tag{1}$$

where m is the mass, k is the stiffness, g is the fractional damping coefficient and D^{α} is the Riemann–Liouville fractional derivative operator defined as

$$D^{\alpha}y(t) = \frac{1}{\Gamma(1-\alpha)}\int_0^t \frac{\dot{y}(\tilde{t})}{(t-\tilde{t})^{\alpha}}d\tilde{t}. \tag{2}$$

The *fractional exponent* α is assumed to be in the range $[0,1]$. The two limiting cases correspond to a viscous damping ($\alpha = 1$) and to a stiffness term ($\alpha = 0$). The stationary external forcing is specified through its power spectral density function $S_f(\omega)$ and is assumed to vary on a slow timescale, compared to the dynamics of the structure. This condition is formalized in the sequel. In wind engineering, such a slow loading is typically attributable to the buffeting loading for which several models exist [39]. For instance, one such model reads

$$S_f\left(\omega; \frac{U}{L}\right) = \sigma_f \frac{0.546\frac{L}{U}}{\left(1+1.64\frac{L}{U}|\omega|\right)^{5/3}} \tag{3}$$

where U and L respectively correspond to the mean wind velocity and the turbulence length scale. The ratio U/L is a small characteristic frequency that is typical of buffeting excitations [40]. This power spectral density model is used in the following illustrations. This is just an example; any other low-frequency excitation could be used to illustrate the following developments.

A dimensionless version of the governing equation is obtained by introducing the characteristic time and the characteristic response

$$t^{\star} = \sqrt{\frac{m}{k}} \qquad \text{and} \qquad y^{\star} = \frac{\sigma_f}{k} \tag{4}$$

and by defining the dimensionless time τ and the scaled response $x(\tau)$ as

$$\tau = \frac{t}{t^{\star}} \qquad \text{and} \qquad x(\tau) = \frac{y(t^{\star}\tau)}{y^{\star}}. \tag{5}$$

Noticing that $D^{\alpha}y(t^{\star}\tau) = y^{\star}t^{\star-\alpha}D^{\alpha}x(\tau)$, the governing equation becomes

$$x''(\tau) + 2\xi D^{\alpha}x(\tau) + x(\tau) = u(\tau) \tag{6}$$

where the prime symbol denotes derivatives with respect to τ, where

$$\xi = \frac{g}{2k\,t^{\star\alpha}} = \frac{g}{2m\,t^{\star\alpha-2}} \tag{7}$$

is the dimensionless *fractional coefficient* and where $u(\tau) = f(\tau t^{\star})/\sigma_f$ is the unit-variance dimensionless external forcing whose power spectral density is given by $S_u(\Omega) = S_f(\Omega/t^{\star})/\sigma_f^2 t^{\star}$ as a function of the dimensionless frequency $\Omega = 2\pi/\tau$ (notice that this non-dimensionalization needs to be reviewed in case of white noise loading, in that case, σ_f can be replaced by $S_f^{1/2}/t^{\star}$). The dimensionless version of the power spectral density of the loading given in (3) reads

$$S_u(\Omega;\beta) = \frac{1}{t^{\star}}S_f\left(\frac{\Omega}{t^{\star}};\frac{\beta}{t^{\star}}\right) = \frac{0.546}{\beta\left(1+1.64\frac{|\Omega|}{\beta}\right)^{5/3}} \tag{8}$$

with $\beta = Ut^{\star}/L \ll 1$ the dimensionless characteristic frequency of the turbulence velocity. Again, we repeat this is just an example and any other loading characterized by power spectral densities whose frequency content is centered on a small frequency β would perfectly fit the scope of this paper.

The Fourier transform of (6) reads

$$\left(1+2\xi C|\Omega|^{\alpha} - \Omega^2 - 2\xi i S|\Omega|^{\alpha}\right)X(\Omega) = U(\Omega) \tag{9}$$

where $C = \cos\frac{\alpha\pi}{2}$ and $S = \sin\frac{\alpha\pi}{2}$, so that the power spectral density of the response is given by

$$S_x(\Omega) = \frac{S_u(\Omega)}{\left(1+2\xi C|\Omega|^{\alpha} - \Omega^2\right)^2 + \left(2\xi S|\Omega|^{\alpha}\right)^2} := K(\Omega)S_u(\Omega). \tag{10}$$

In this expression, we have defined the kernel (frequency response function) $K(\Omega)$ of this problem. It is illustrated in Fig. 1 for several values of α. It has some peculiarities: (i) the resonance peak located near $\Omega = \pm 1$ in the viscous case ($\alpha = 1$) regularly moves to higher frequencies as $\alpha \to 0$, i.e. as the fractional derivative term tends to correspond to a stiffness term. In the limiting case $\alpha = 0$, the fractional derivative corresponds to a usual stiffness term and the peak is located at abscissa $\Omega_p = \sqrt{1+2\xi} \simeq 1+\xi$; (ii) the frequency response function passes through a common *crossing point*, at abscissa $\Omega = 1$, no matter the fractional exponent α (this is readily observed by replacing Ω by 1 in the definition of the kernel); (iii) in the range $\Omega \in [-1;1]$ the kernel is comprised in the area generated by the two limiting cases $\alpha = \{0,1\}$ with $\alpha = 0$ being the lower bound and $\alpha = 1$ being the upper bound; (iv) the coordinate at the origin is $K(0) = 1$ provided $\alpha \neq 0$. As $\alpha \to 0$, a short boundary layer, whose extent is of order α, develops in the neighborhood of the origin and creates the transition from the upper bound $K(0) = 1$ to the lower bound $K(\Omega) \simeq \frac{1}{(1+2\xi)^2}$. For $\alpha \to 0$, the size of this transition zone tends to zero; for $\alpha = 0$, there is no transition anymore and $K(0) = \frac{1}{(1+2\xi)^2}$.

As a result of the fractional powers of Ω appearing in $K(\Omega)$, the response of the system, its variance, defined as

$$\sigma_x^2 = \int_{-\infty}^{+\infty} S_x(\Omega)d\Omega, \tag{11}$$

is unfortunately not available in a simple closed form, even for simple forms of the power spectral density of $u(\tau)$.

In the sequel we assume that $\xi \ll 1$. This is very similar to the developments based on stochastic averaging, van der Pol transformations, quasi-Hamiltonian systems and the likes and results in three timescales in the problem : (i) the slow timescale of the loading β^{-1}, (ii) the slow timescale associated with the energy of the system ξ^{-1} and (iii) the fast (unit) timescale associated with the phase of the system. Unlike existing approaches exploiting the smallness of ξ in the time domain, we also recognize the existence of the different scales and exploit it, but in the frequency domain. As shown next, this allows a very simple derivation of the approximate solution of the problem. The method is based on the Multiple Timescale Spectral Analysis, which is briefly summarized before tackling the problem at hand.

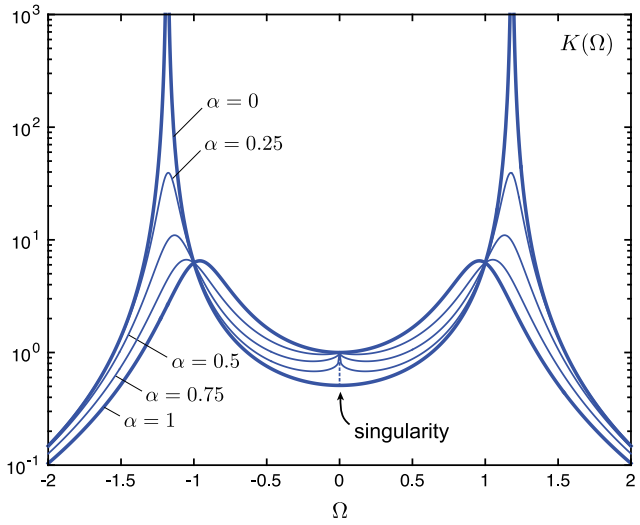

Fig. 1. Representation of the kernel $K(\Omega)$ for various values of the fractional exponent α. Other parameters: $\xi = 0.2$.

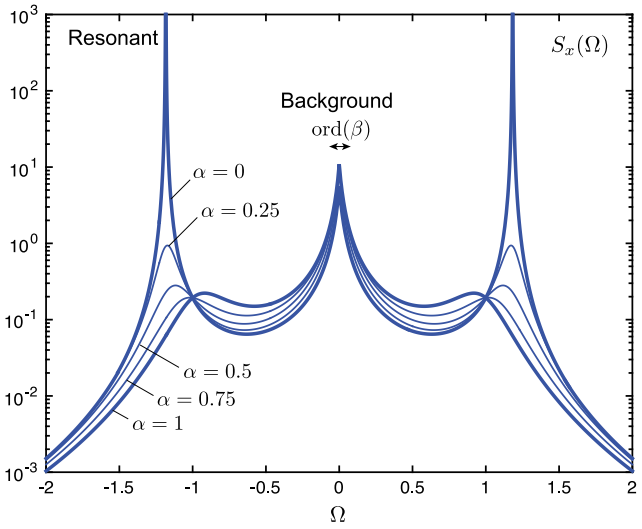

Fig. 2. Examples of the power spectral density of the structural response for various values of the fractional exponent α. Other parameters: $\xi = 0.2$, $\beta = 0.05$.

3. Multiple timescale spectral analysis

The multiple timescale spectral analysis is a general framework developed to derive approximate responses of stochastic systems involving various well separated timescales [33]. In this paper, we only need the steady-state 1-D version of the method, which is summarized as follows. Let us consider a (linear, for the sake of this study; but it could be slightly nonlinear) structural system subjected to a stationary stochastic input. The steady-state variance of the response is given by

$$\sigma_x^2 = \int_{-\infty}^{+\infty} K(\Omega) S_u(\Omega) d\Omega. \tag{12}$$

Instead of the numerical computation of this integral, one might be interested in an approximate closed form expression, by taking advantage of the timescale separation. To do so, the multiple timescale spectral analysis consists first in identifying all different contributions to the integral. They might be either global, i.e. on a domain of order 1 or more, or local in which case they look like a peak over a short domain. The existence of one or several small numbers in the problem might be used to justify the distinctness of the peaks and is useful to estimate the order of magnitude of each contribution. In a second step, these contributions to the integral are evaluated, in a sequential manner, starting with the domain or peak that contributes the most to the integral. This evaluation develops in several steps: (i) provide a local approximation $\hat{K}(\Omega)\hat{S}_u(\Omega)$ of the integrand $K(\Omega)S_u(\Omega)$ that is accurate over the considered domain or peak, and that drops to zero in the far field, in order to be integrable (this condition is very similar to the management of Poincaré's secular terms in the time domain version of the multiple timescale method). This approximation should also be simple enough so that the integral

$$\sigma_{x,1}^2 = \int_{-\infty}^{+\infty} \hat{K}(\Omega)\hat{S}_u(\Omega) d\Omega \tag{13}$$

corresponding to the first contribution might be evaluated in an explicit way; (ii) once this is done, subtract (13) from (12), in order to obtain a remainder $r_1 = \sigma_x^2 - \sigma_{x,1}^2$ which is evaluated as the integral of $K(\Omega)S_u(\Omega) - \hat{K}(\Omega)\hat{S}_u(\Omega)$. This integrand does not have any significant contribution anymore, in the neighborhood of the peak(s) that has/have already been treated. The sequence then follows with the next contribution. When the process is over, the last remainder is neglected. It provides the order of magnitude of the error committed with the approximation. Please refer to [33] for more details and examples.

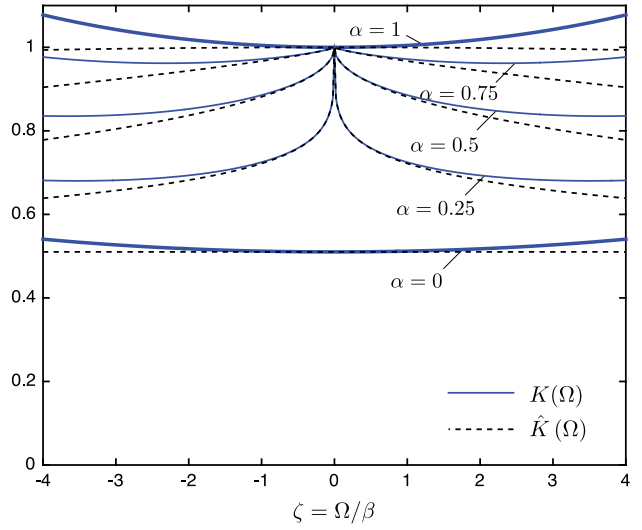

Fig. 3. Local approximation of the kernel in the neighborhood of the origin, represented for various values of the fractional exponent α. Illustration given for $\xi = 0.2$.

4. Solution of the problem and discussion

Fig. 2 shows some examples of the power spectral density of the structural response given by (10). This function features two distinct types of peaks: one in the low-frequency range around $\Omega \simeq 0$ and over a domain whose extent is of order β (the background component) and the other in the order-one frequency range (the resonant component). We successively focus on these two types of peaks in the sequel. They are well distinct because $\beta \ll 1$.

4.1. Background component

Following the general method of the multiple timescale spectral analysis, we first focus on the background component, in the low-frequency range, and define a local approximation of $S_x(\Omega)$. Similarly to what is done for the oscillator with viscous damping [33], only $K(\Omega)$ is approximated. The stretched coordinate ζ, defined as

$$\Omega = \beta\zeta \quad \Longleftrightarrow \quad \zeta = \frac{\Omega}{\beta}$$

is introduced in order to rescale the range $\Omega = \text{ord}(\beta)$ to an order-one interval when $\zeta = \text{ord}(1)$. Using this scaling, the kernel is expressed as

$$K\left[\Omega\left(\zeta\right)\right] = \frac{1}{\left(1 + 2\xi C\beta^{\alpha}|\zeta|^{\alpha} - \beta^2\zeta^2\right)^2 + \left(2\xi\beta^{\alpha}S|\zeta|^{\alpha}\right)^2}. \tag{14}$$

An approximation of this exact kernel is necessary to establish a closed-form expression of the background component. Evoking the smallness of $\beta \ll 1$, while the stretched coordinate ζ is of order 1, we can drop the term $\beta^2\zeta^2$ in the first term of the denominator and approximate the exact kernel by

$$\hat{K}\left[\Omega\left(\zeta\right)\right] = \frac{1}{1 + 4\xi C\beta^{\alpha}|\zeta|^{\alpha} + 4\xi^2\beta^{2\alpha}|\zeta|^{2\alpha}}. \tag{15}$$

This is the frequency response function of a low pass fractional filter [41]. This approximation is represented in Fig. 3, for several values of α. This figure also shows $K\left[\Omega\left(\zeta\right)\right]$ for $\alpha = 0$ and shows that the singular behavior at $\zeta = 0$ is well captured. A Taylor series expansion for β around 0 would certainly not have provided such an accurate approximation. Expression (15) fits the requirements of the multiple timescale spectral analysis since it is seen to be locally accurate even when $\alpha = 0$; furthermore it is bounded in the far field and has a more or less simple analytical expression. Using this approximation, the background component of the response is finally expressed as

$$\sigma_{x,b}^2 = \int_{-\infty}^{+\infty} S_u(\Omega)\hat{K}\left(\Omega\right)d\Omega = \int_{-\infty}^{+\infty} \frac{S_u(\Omega)}{1 + 4\xi C|\Omega|^{\alpha} + 4\xi^2|\Omega|^{2\alpha}}d\Omega. \tag{16}$$

For $\alpha \simeq 1$ and $\xi \ll 1$, this dimensionless background component is a small perturbation of 1 as a result of our choices for the scaling of the problem. The integral in (16) requires numerical integration as soon as $\alpha \neq 1$. We notice however that this integral only depends on the loading parameters ξ and α and is independent of the properties of the dynamical system. This integral could therefore be determined once and for all, for a given loading $S_u(\omega)$.

Nevertheless there are two alternative solutions to avoid the numerical computation of this integral. First, the kernel might be approximated as $\tilde{K}\left(\Omega\right) \simeq 1$ and the background component could be approximated as

$$\tilde{\sigma}_{x,b}^2 = \int_{-\infty}^{+\infty} S_u(\Omega)d\Omega = 1. \tag{17}$$

This approximation is much simpler, consistent with viscous damping [33] but does not capture the rapid decrease of the kernel for $\alpha \ll 1$ in the neighborhood of the origin. This is further discussed next.

Instead, driven by the fact the we would like to recover $\hat{K}\left[\Omega\left(\zeta\right)\right] \simeq (1+2\xi)^{-2}$ in the limit case $\alpha = 0$, we could determine a Padé approximant (a rational fraction approximation in ξ) by redefining $\hat{K}\left[\Omega\left(\zeta\right)\right]$ as $(1 + 2\xi)^{-2}$ multiplied by the series expansion of $(1 + 2\xi)^2\hat{K}\left[\Omega\left(\zeta\right)\right]$. For consistency, this series is truncated after the second term. After some developments, this results in the new approximation

$$\overline{K}(\Omega) = \frac{1 + 4\xi\left(1 - C|\Omega|^{\alpha}\right) + 4\xi^2\left(1 - 4C|\Omega|^{\alpha} - (1 - 4C^2)|\Omega|^{2\alpha}\right)}{(1 + 2\xi)^2} \tag{18}$$

which yields

$$\bar{\sigma}_{x,b}^2 = \int_{-\infty}^{+\infty} S_u(\Omega)\overline{K}\left(\Omega\right)d\Omega = 1 - \frac{4\xi C\left(1 + 4\xi\right)}{(1 + 2\xi)^2}m_{u,\alpha} - \frac{4\xi^2(1 - 4C^2)}{(1 + 2\xi)^2}m_{u,2\alpha} \tag{19}$$

where $m_{u,\alpha} = \int_{-\infty}^{+\infty} S_u(\Omega)|\Omega|^{\alpha}d\Omega$ is the α-fractional spectral moment of $S_u(\Omega)$. Depending on the high-frequency behavior of the external forcing, its α- and 2α-fractional spectral moments might not be defined. In case one of them (or even $m_{u,0} = 1$, the first term in the expression) is unbounded, they should not be included in the expression of the background component. This other approximation is interesting but has limited applicability for this reason.

In the following section, we continue the derivation with the more accurate expression $\sigma_{x,b}^2$ defined in (16).

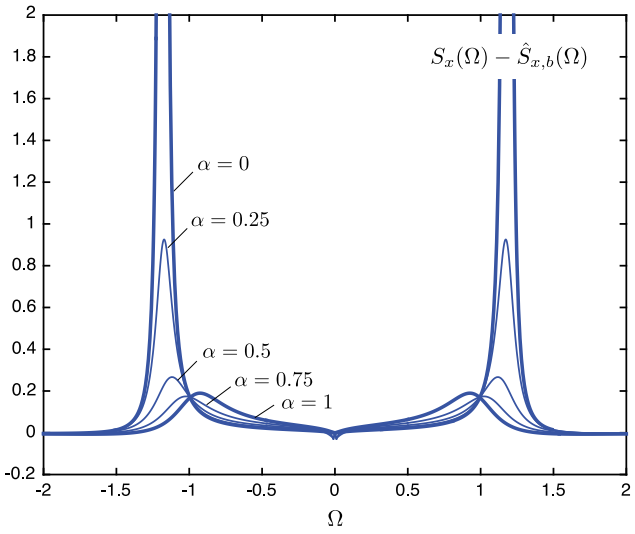

Fig. 4. Remainder after subtraction of the background component, represented for various values of the fractional exponent α. Other parameters: $\xi = 0.2$, $\beta = 0.05$.

4.2. Resonant component

The remainder is obtained by subtracting this first approximation from the original function to integrate, that is

$$r_1 = \int_{-\infty}^{+\infty} S_x(\Omega) - S_u(\Omega)\hat{K}\left(\Omega\right)d\Omega = \int_{-\infty}^{+\infty} S_u(\Omega)\left(K\left(\Omega\right) - \hat{K}\left(\Omega\right)\right)d\Omega. \tag{20}$$

The function to be integrated features two symmetrical peaks which will equally contribute the resonant part of the response. They first need to be accurately localized, at least in terms of orders of magnitude. In a second step, the local approximation will be derived (see Fig. 4).

Assuming that the power spectral density of the loading varies smoothly in the neighborhood of the peaks of the frequency response function of the system (located at $\pm\Omega_p$), the peaks in the response are located at the same abscissa as the peaks in the kernel. The actual position of these peaks is then obtained by canceling the first derivative of the denominator of the kernel $K(\Omega)$. It is therefore given by

$$\Omega_p\left(1 + 2\xi C\left|\Omega_p\right|^{\alpha} - \Omega_p^2\right)\left(\alpha\xi C\left|\Omega_p\right|^{\alpha-2} - 1\right) + 2\alpha\xi^2S^2\left|\Omega_p\right|^{2\alpha-1} = 0. \tag{21}$$

Unfortunately, because of the fractional derivatives, this expression does not accept any explicit solution. Instead, we take advantage of the smallness of ξ and use the first iteration of an iterative scheme [42] to obtain an approximation of the root. Initializing the iterative scheme with $\Omega_{(1)} = 1$, defining the iterative scheme by

$$\Omega_{(k)}\left(1 + 2\xi C\left|\Omega_{(k)}\right|^{\alpha} - \Omega_{(k+1)}^2\right)\left(\alpha\xi C\left|\Omega_{(k)}\right|^{\alpha-2} - 1\right) + 2\alpha\xi^2S^2\left|\Omega_{(k)}\right|^{2\alpha-1} = 0 \tag{22}$$

and retaining the positive root, we obtain an explicit solution for $\Omega_{(2)}$

$$\Omega_{(2)} = \left(1 + 2\xi C + \frac{2\alpha\xi^2S^2}{\alpha\xi C - 1}\right)^{1/2}. \tag{23}$$

The Maclaurin series expansion of that solution for ξ yields an explicit approximation of the position of the peak $\Omega_p \simeq \Omega_{(2)}$ that reads

$$\Omega_p = 1 + C\xi - \left[\alpha + \left(\frac{1}{2} - \alpha\right)C^2\right]\xi^2 + \mathcal{O}(\xi^2). \tag{24}$$

The position of the peak is a perturbation of 1 (again, as a result of the scaling). The peak in $\mathbb{R}^-$ is symmetrically located. For $\alpha \simeq 1$, the

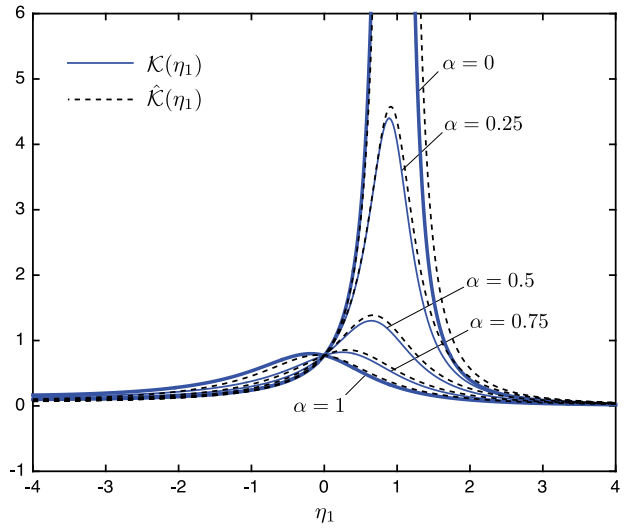

Fig. 5. Remainder after subtraction of the background component, represented for various values of the fractional exponent α. Other parameters: $\xi = 0.2$, $\beta = 0.05$.

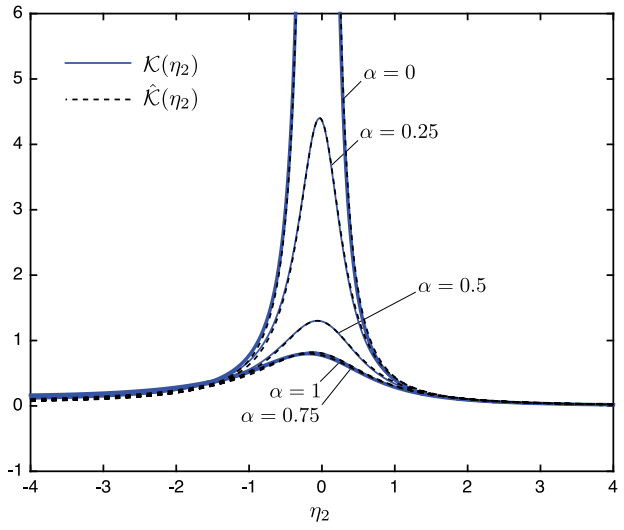

Fig. 6. Remainder after subtraction of the background component, represented for various values of the fractional exponent α. Other parameters: $\xi = 0.2$, $\beta = 0.05$.

fractional derivative resembles a viscous effect, $C = \cos\frac{\alpha\pi}{2} \ll 1$ and the position of the peak is very close to $1 - \xi^2$, the peak of the viscously damped system. For $\alpha \simeq 0$, $C \simeq 1$ and the position of the peak is located close to abscissa $1 + \xi$; this is consistent with what has been announced earlier. This is also consistent with existing results obtained with a stochastic averaging approach, at least at leading order in ξ [16].

Now that the position of the peak is determined, we can introduce a stretched coordinate η to focus on the resonant contribution to the response. It is expected that the more accurate the localization of the peak, the more accurate the final solution. However, to make the solution more accurate has a certain cost and it might not be optimal to keep a second-order accurate solution in ξ. In this paper we will develop two solutions in parallel: in the first one, we assume that the position of the peak is located at $\Omega_p = 1$ while, in the second, we assume that the position of the peak is located at $\Omega_p = 1 + C\xi$, which is more accurate but results in longer expressions, at least during the developments.

In the first case, the stretched coordinate η_1 is naturally chosen as

$$\Omega = 1 + \xi\eta_1 \quad \Longleftrightarrow \quad \eta_1 = \frac{\Omega - 1}{\xi}$$

while in the latter, it is chosen as

$$\Omega = 1 + C\xi + \xi\eta_2 \quad \Longleftrightarrow \quad \eta_2 = \frac{\Omega - 1 - C\xi}{\xi}.$$

With the first stretching, the factor in the parenthesis in (20) becomes after some simplifications

$$\mathcal{K}(\eta_1) := \frac{1}{4\xi^2}\frac{1}{\eta_1^2(1+\frac{1}{2}\eta_1\xi)^2 + (1+\eta_1\xi)^{2\alpha} - C\eta_1(2+\xi\eta_1)(1+\xi\eta_1)^{\alpha}} - \hat{K}\left[\Omega\left(\eta_1\right)\right]. \tag{25}$$

No matter the chosen approximation for the background component ($\sigma^2_{x,b}$ or $\tilde{\sigma}^2_{x,b}$), the last term might be dropped since it is composed of terms which are two to three orders of magnitude smaller than the first term. Further considering that $\eta_1\xi \ll 1$, we can derive an approximation for the new kernel that reads

$$\hat{\mathcal{K}}(\eta_1) := \frac{1}{4\xi^2}\frac{1}{\eta_1^2 - 2C\eta_1 + 1}. \tag{26}$$

Notice that we could easily get rid of the fractional powers. This approximation is simple, locally accurate (for $\eta_1 = \text{ord}(1)$) and bounded in the far field. Fig. 5 shows a comparison of the exact integrand $\mathcal{K}(\eta_1)$ in the remainder and this first approximation. The corresponding approximation of the remainder is

$$\hat{r}_1 = \int_{-\infty}^{+\infty} S_u\left[\Omega\left(\eta_1\right)\right]\hat{\mathcal{K}}(\eta_1)\xi d\eta_1 \tag{27}$$

which is further simplified by assuming that $S_u\left[\Omega\left(\eta_1\right)\right]$ does not vary significantly in the neighborhood of $\eta_1 = \text{ord}(1)$, which yields

$$\hat{r}_1 = S_u(1)\int_{-\infty}^{+\infty}\hat{\mathcal{K}}(\eta_1)\xi d\eta_1 = \frac{S_u(1)}{4S\xi}\left[\arctan\left(\frac{\eta_1+1}{\eta_1-1}\tan\frac{\alpha\pi}{4}\right)\right]_{-\infty}^{+\infty} = \frac{\pi S_u(1)}{4S\xi}. \tag{28}$$

The resonant component of the response is then obtained by multiplying this approximation by 2, in order to account for the two symmetrical peaks,

$$\tilde{\sigma}^2_{x,r} = \frac{\pi S_u(1)}{2S\xi}. \tag{29}$$

For $\alpha \simeq 1$, the fractional derivative term in the governing equation resembles a viscous damping, $S \simeq 1$, and the resonant term corresponds to the well-known response of a linear viscous oscillator subject to white noise excitation [43]. For $\alpha \simeq 0$, the fractional derivative term resembles a stiffness term, in which case the considered problem tends to an undamped oscillator which is known to have no steady state solution and requires being studied with other approaches [44,45]. The approximation in (29) is therefore very simple and compact and recovers some well-known limiting cases. As anticipated before, it might however be inaccurate when $\alpha \to 0$ since the location of the peak might be too different from 1, which was the assumption to derive this first solution.

Using the second stretching, the factor in the parenthesis in (20) becomes after dropping the last term (for same reason as before)

$$\mathcal{K}(\eta_2) := \frac{1}{4\xi^2}\left[\left[C\left(1+C\xi+\xi\eta_2\right)^{\alpha} - \left(1+\frac{1}{2}C\xi+\frac{1}{2}\xi\eta_2\right)\left(C+\eta_2\right)\right]^2 + S^2\left(1+C\xi+\xi\eta_2\right)^{2\alpha}\right]^{-1}. \tag{30}$$

Expanding the square and using the binomial theorem stating that $(1+\epsilon)^{\alpha} = 1 + \alpha\epsilon + \text{ord}(\epsilon^2)$

$$\mathcal{K}(\eta_2) := \frac{1}{4\xi^2}\left[\left(1+\frac{1}{2}C\xi+\frac{1}{2}\xi\eta_2\right)^2\left(C+\eta_2\right)^2 + \left(1+2\alpha C\xi+2\alpha\xi\eta_2\right) - 2C\left(1+\alpha C\xi+\alpha\xi\eta_2\right)\left(1+\frac{1}{2}C\xi+\frac{1}{2}\xi\eta_2\right)\left(C+\eta_2\right)\right]^{-1}. \tag{31}$$

This expression of the kernel is still a little too long and might require further simplification. The denominator of $\mathcal{K}(\eta_2)$ is a fourth order polynomial in η_2, which yields four poles in the complex plane and the two peaks located at $\Omega = \pm\Omega_p$ on the real axis. A much better job is done by focusing on one peak at a time. To do so, we are free to drop the degree of the polynomial from 4 to 2, by discarding all terms of the denominator involving third and fourth powers of η_2, and making sure only one peak on the real axis remains. This approach is similar to what was done with the first stretching when simplifying (25) into (26); it is also deeply discussed in [33].

After a bit of standard algebra and some simplifications, we finally obtain the local approximation

$$\hat{\mathcal{K}}(\eta_2) := \frac{1}{4\xi^2}\frac{1}{c_2\eta_2^2 + c_1\eta_2 + c_0} \tag{32}$$

where the coefficients $c_0 = S^2(1 + 2\xi\alpha C)$, $c_1 = \frac{1}{2}\xi(1 + (1-4\alpha)(1-2S^2))$ and $c_2 = 1 + 2\xi(1-\alpha)C$ are truncated to their first order terms in their respective Maclaurin series expansion for ξ. This approximation is a little bit more complicated than (26) but has a somewhat similar format. However, as $\alpha \to 1$, i.e. $C \to 0$ and $S \to 1$, coefficients c_0, c_1 and c_2 respectively tend to 1, 2ξ and 1 which is slightly different from the coefficients 1, $-2C$ and 1 in $\hat{\mathcal{K}}(\eta_1)$. This difference should be manageable as long as both ξ and C remain small (compared to one); it also highlights the limitations of the first approximation.

Fig. 6 shows $\mathcal{K}(\eta_2)$ and $\hat{\mathcal{K}}(\eta_2)$. As expected, with this second stretching, the peaks in the stretched coordinate system are almost centered on $\eta_2 = 0$ no matter the value of the fractional exponent α, while the first stretching provides peaks centered on $\eta_1 = 0$ only as $\alpha \to 1$. Also, the integrand and the local approximation are virtually superimposed in the range $[-4, 4]$, which announces an accurate result.

Assuming again that the power spectral density of the loading does not significantly vary in the neighborhood of $\Omega = \Omega_p$, the corresponding approximation of the remainder is

$$\begin{aligned}\hat{r}_1 &= S_u(1+C\xi)\int_{-\infty}^{+\infty}\hat{\mathcal{K}}(\eta_2)\xi d\eta_2 = \frac{S_u(1+C\xi)}{4\xi^2}\xi\left[\frac{2}{\rho}\arctan\frac{c_1+2c_2\eta}{\rho}\right]_{-\infty}^{+\infty}\\ &= \frac{\pi S_u(1+C\xi)}{2\rho\xi}\end{aligned} \tag{33}$$

where $\rho = \sqrt{4c_0c_2 - c_1^2} = \left[4(1+2\xi C)S^2 + \text{ord}\left(\xi^2\right)\right]^{1/2}$. Truncating again ρ to its leading order terms, and multiplying $\hat{r}_1$ by 2 to take both peaks into account, the resonant contribution to the response finally reads

$$\sigma_{x,r}^2 = \frac{\pi S_u(1+C\xi)}{2S\xi\sqrt{1+2\xi C}}. \tag{34}$$

This approximation is slightly richer than (29) in the sense that (29) was not designed for α different from 1 (i.e. C different from 0), while (34) was designed to provide an approximation in the more general case. Because (34) is not much more complicated than (29), it is naturally recommended to use (34) and consider $\tilde{\sigma}_{x,r}^2$ as a (simpler) variant of the resonant contribution. The only major difference is that the algebra required to establish (34) was a bit more involved.

4.3. Summary

To summarize, the background/resonant decomposition of the variance of a linear oscillator with fractional derivatives is given by

$$\begin{aligned}\sigma_x^2 &= \sigma_{x,b}^2 + \sigma_{x,r}^2\\ &= \int_{-\infty}^{+\infty}\frac{S_u(\Omega)}{1+4\xi C|\Omega|^\alpha + 4\xi^2|\Omega|^{2\alpha}}d\Omega + \frac{\pi S_u(1+C\xi)}{2S\xi\sqrt{1+2\xi C}}.\end{aligned} \tag{35}$$

We have also derived two variants, one for the background and one for the resonant components. The variant for the background, $\tilde{\sigma}_{x,b}^2 = 1$, although a little less accurate than $\sigma_{x,b}^2$ might prove interesting since it avoids the computation of the fractional low passed energy of the loading $u(t)$. The variant for the resonant component $\tilde{\sigma}_{x,r}^2$ is not much simpler but was obtained with a simpler derivation. It is not really worth being considered in practical applications.

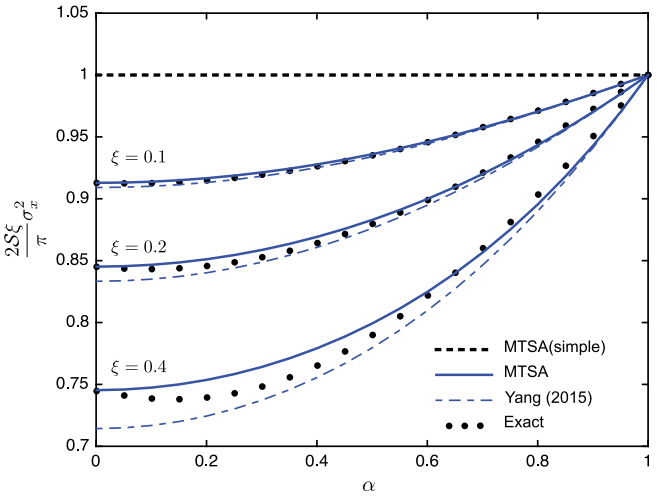

Fig. 7. Variance of the response of a fractional oscillator subjected to a unit white noise excitation. (Please see online version for colors).

Substituting back with the original variables of the problem

$$\sigma_y^2 = \frac{1}{k^2}\int_{-\infty}^{+\infty}\frac{S_f(\omega_0)\,\mathrm{d}\omega}{1+4\xi C\left|\frac{\omega}{\omega_0}\right|^\alpha + 4\xi^2\left|\frac{\omega}{\omega_0}\right|^{2\alpha}} + \frac{1}{k^2}\frac{\pi\omega_0 S_f\left[\omega_0(1+C\xi)\right]}{2S\xi\sqrt{1+2\xi C}} \tag{36}$$

where $\omega_0 = 1/t^\star = \sqrt{k/m}$ is the natural circular frequency of the undamped system.

5. Validation, illustrations and discussion

The accuracy of the proposed formulation will be assessed by comparison with the exact result. The exact result is obtained by numerical integration of the exact power spectral density of the response. Integration is performed with the adaptive algorithm proposed in Wolfram Mathematica [46], with default integration parameters of Version 11.0.1.0.

5.1. Validation: white noise excitation

As a validation case, the response of an oscillator equipped with a viscoelastic device and subjected to a delta correlated excitation is considered. This problem has already been tackled with a stochastic averaging approach, e.g. [16]. Both the stochastic averaging and the multiple timescale spectral analysis are based on the same assumption that the damping ratio (or fractional coefficient ξ) is a small parameter. To compare them both therefore borders more on the confrontation than validation, which is considered in a second step by comparison with the exact solution.

In the multiple timescale spectral analysis (MTSA) formulation, the background component needs to be discarded, since the variance of the delta-correlated noise is infinite. We are therefore left with the resonant component $\sigma_{x,r}^2$ (or $\tilde{\sigma}_{x,r}^2$) where $S_u(1+C\xi)$ is replaced by 1, which yields

$$\frac{2S\xi}{\pi}\sigma_x^2 = \frac{1}{\sqrt{1+\xi C}} \quad \text{or} \quad \frac{2S\xi}{\pi}\tilde{\sigma}_x^2 = 1, \tag{37}$$

while the approximation derived in [16] reads, with our notations,

$$\frac{2S\xi}{\pi}\sigma_x^2 = \frac{1}{1+\xi C}. \tag{38}$$

First, we recognize that all three approximations have the same leading order behaviors in ξ and α, which are expressed by the leading product

$S\xi$, repelled to the left-hand side. The slight differences on the right-hand side are therefore associated with the second order terms. This is a first validation of the appropriateness of the solutions we have developed, since it recovers the same leading order solution as the reputed stochastic averaging response. Fig. 7 shows these three results (the right-hand side) and provides a comparison with the exact result, represented with back dots. In all cases, the simple MTSA formulation fails to finely capture the second-order dependency in α. For $\xi = 0.1$, both the MTSA and the stochastic averaging (Yang 2015) formulations are almost perfect. For larger fractional coefficients, $\xi = 0.2$ and $\xi = 0.4$, these two solutions capture the right trend but are naturally much less accurate, since they are developed under the assumption $\xi \ll 1$. However the multiple timescale spectral analysis method recovers the exact result in the limit case $\alpha = 0$, while the stochastic averaging is consistently underestimating the exact result.

5.2. Illustration: buffeting type excitation

The governing equation (6) is now considered together with the buffeting loading described by (8). Figs. 8 and 9 show the variance of the response obtained with the proposed formulation (MTSA) and by numerical integration of the exact analytical formulation. The variance is represented as a function of α for given values of ξ, and as a function of ξ for given values of α. In both figures, the background component $\sigma^2_{x,b}$ is shown with dashed lines. This is to illustrate two facts: (i) the smaller ξ and the larger α, the better the approximation $\tilde{\sigma}^2_{x,b} = 1$; this approximation seems reasonable for $\xi \lesssim 10^{-2}$ (ii) the behavior of the system is quasi-static for large ξ or large α, since the total variance (MTSA) is very close to the background component in those areas.

For $\beta = 0.01$ (on the left), the proposed approximation provides a very accurate estimation of the variance of the response, throughout the different scales of ξ and over the whole range $[0, 1]$ for α. Fig. 10 represents the relative error realized with the proposed approximation and indeed confirms that the error remains smaller than 1% for $\xi < 10^{-2}$, no matter the value of α. The contours of the error curve up for small values of α which is, again, a consequence of the accuracy of the resonant component (the only one that matters as $\alpha \to 0$) in this limit case. The central plot in Fig. 10 shows the relative error obtained with the approximation $\tilde{\sigma}^2_{x,b} + \sigma^2_{x,r}$, i.e. by changing the way the background contribution is computed. As expected, for $\xi \lesssim 10^{-2}$, the response is mostly resonant and the error is not affected by the way the background component is estimated. For $\xi > 10^{-2}$, the response is mostly quasi-static and the background component is more important. In that case, the error grows slightly more proportionally than ξ. On the right, Fig. 10 shows the relative error obtained with the approximation $\tilde{\sigma}^2_{x,b} + \tilde{\sigma}^2_{x,r}$. In that case, both the background and the resonant components are too roughly estimated. This results in errors of a few percents as soon as $\xi > 5 \cdot 10^{-3}$.

6. Conclusions

In this paper, we have applied the multiple timescale spectral analysis to the structural analysis of a linear system equipped with a viscoelastic device. Compared to the well-known solution of the linear viscous problem, it has been shown that the background component requires a little more attention, especially as soon as the fractional coefficient ξ is larger than or similar to 10^{-2}. In that case, a low pass fractional filter of the excitation needs to be considered to establish the background component. The resonant component of the response is also

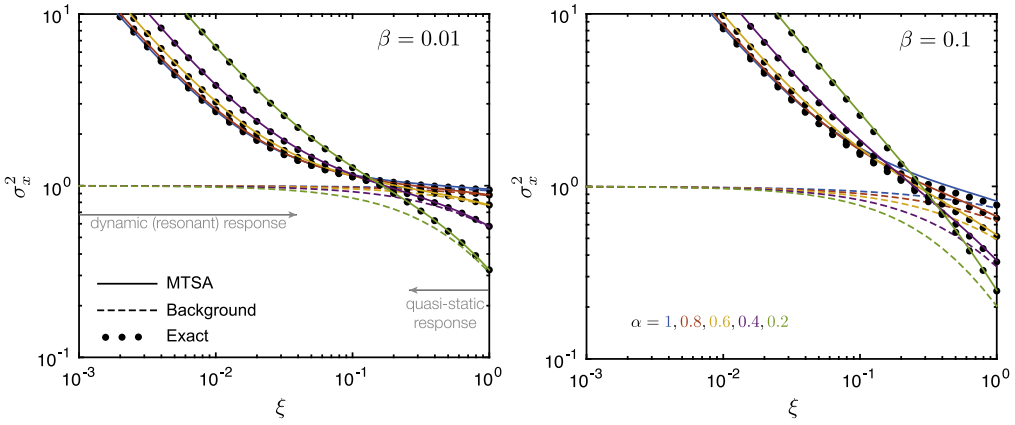

Fig. 8. Variances of the response of the system subjected to the buffeting type excitation, for $\beta = 0.01$ (left) and $\beta = 0.1$ (right). Represented as a function of the fractional coefficient ξ and for various values of the fractional exponent α. (Please see online version for colors).

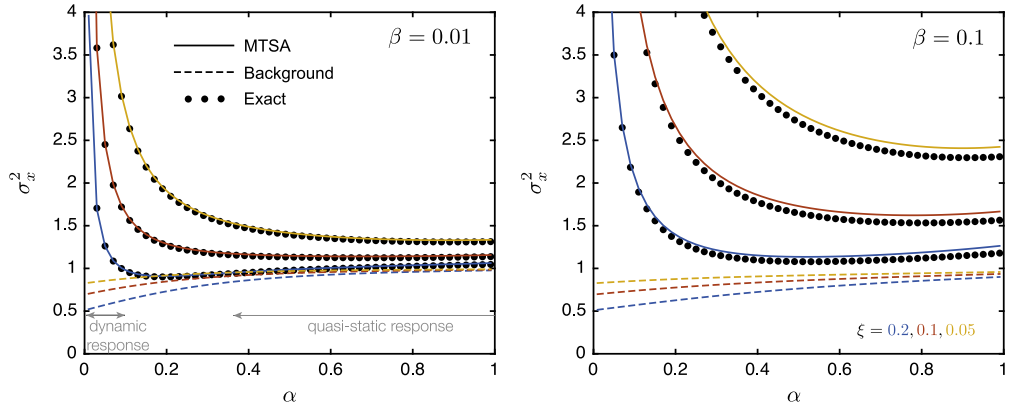

Fig. 9. Variances of the response of the system subjected to the buffeting type excitation, for $\beta = 0.01$ (left) and $\beta = 0.1$ (right). Represented as a function of the fractional exponent α and for various values of the fractional coefficient ξ. (Please see online version for colors).

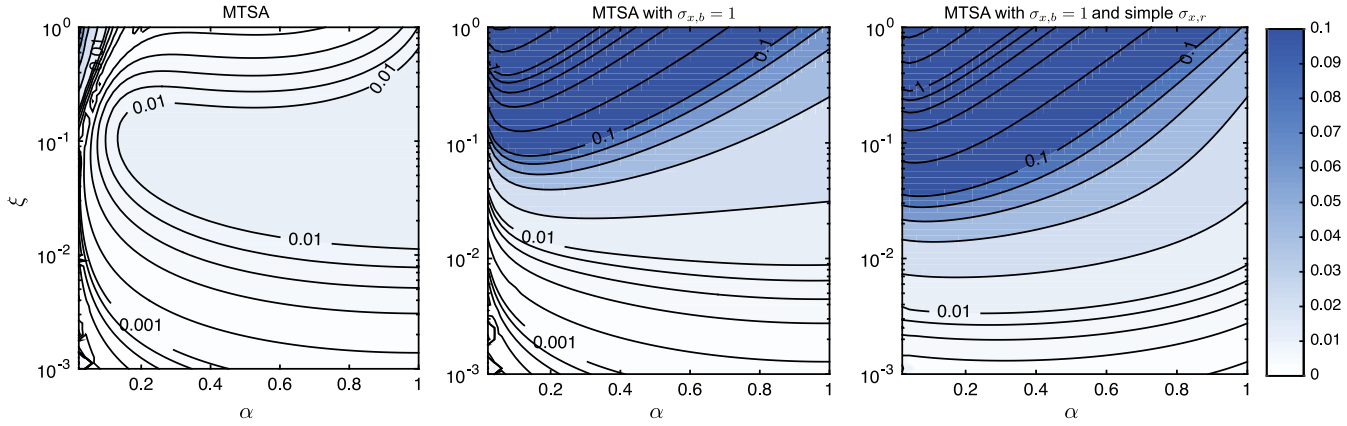

Fig. 10. Relative error on the variance of the response of a fractional oscillator subjected to a low frequency turbulent loading, as a function of the fractional exponent α and the fractional coefficient ξ. (Please see online version for colors).

affected by the presence of the viscoelastic device. At first order, it is simply obtained by dividing the classical response in the viscous case by $\mathcal{S} = \sin\frac{\alpha\pi}{2}$. Several solutions have been proposed and discussed. Among them, (35)–(36) should be preferred.

The game of stretching and rescaling that rules the multiple timescale spectral analysis offers more flexibility to derive approximate solutions than standard time-domain methods. The resulting approximation might not necessarily be optimal, in one (or some) sense, but at least may features interesting advantages. For instance, the proposed solution is shown to provide more accurate results than those obtained with the stochastic averaging method, as the fractional exponent $\alpha \to 0$.

Extrapolating on these promising results, further works should extend to slightly nonlinear or multiple degree-of-freedom structures.

References

[1] C. Ionescu, A. Lopes, D. Copot, J.A.T. Machado, J.H.T. Bates, The role of fractional calculus in modeling biological phenomena: A review, Commun. Nonlinear Sci. Numer. Simul. 51 (2017) 141–159.

[2] R.L. Magin, Fractional Calculus in Bioengineering, Begell House Publishers, 2006.

[3] Y. Hu, B. Oksendal, Fractional white noise calculus and applications to finance, Infin. Dimens. Anal. Quantum Probab. Relat. Top. 06 (01) (2003) 1–32.

[4] N. Makris, M.C. Constantinou, Fractional-derivative Maxwell model for viscous dampers, J. Struct. Eng. 117 (9) (1991) 2708–2724.

[5] W. Sun, Z. Wang, X. Yan, M. Zhu, Inverse identification of the frequency-dependent mechanical parameters of viscoelastic materials based on the measured FRFs, Mech. Syst. Signal Process. 98 (2018) 816–833.

[6] M. Grigoriu, Linear systems with fractional Brownian motion and Gaussian noise, Probab. Eng. Mech. 22 (3) (2007) 276–284.

[7] P.D. Spanos, B.A. Zeldin, Random vibration of systems with frequency-dependent parameters or fractional derivatives, J. Eng. Mech. 123 (3) (1997) 290–292.

[8] L. Chen, F. Hu, W. Zhu, Stochastic dynamics and fractional optimal control of quasi integrable Hamiltonian systems with fractional derivative damping, Fract. Calc. Appl. Anal. 16 (1) (2013) 189–225.

[9] O.P. Agrawal, Stochastic analysis of dynamic systems containing fractional derivatives, J. Sound Vib. 247 (5) (2001) 927–938.

[10] R.L. Bagley, P.J. Torvik, Fractional calculus in the transient analysis of viscoelastically damped structures, AIAA J. 23 (6) (1985) 918–925.

[11] A. Palmeri, F. Ricciardelli, G. Muscolino, A. De Luca, Random vibration of systems with viscoelastic memory, J. Eng. Mech. 130 (9) (2004) 1052–1061.

[12] M. Di Paola, G. Failla, A. Pirrotta, Stationary and non-stationary stochastic response of linear fractional viscoelastic systems, Probab. Eng. Mech. 28 (2012) 85–90.

[13] L. Chen, W. Wang, Z. Li, W. Zhu, Stationary response of Duffing oscillator with hardening stiffness and fractional derivative, Int. J. Non-Linear Mech. 48 (2013) 44–50.

[14] Z.L. Huang, X.L. Jin, C.W. Lim, Y. Wang, Statistical analysis for stochastic systems including fractional derivatives, Nonlinear Dynam. 59 (1) (2010) 339–349.

[15] Y. Yang, W. Xu, X. Gu, Y. Sun, Stochastic response of a class of self-excited systems with Caputo-type fractional derivative driven by Gaussian white noise, Chaos Solitons Fractals 77 (2015) 190–204.

[16] Y. Yang, W. Xu, W. Jia, Q. Han, Stationary response of nonlinear system with Caputo-type fractional derivative damping under Gaussian white noise excitation, Nonlinear Dynam. 79 (1) (2015) 139–146.

[17] J.-F.A. Zhao, Stochastic response of dynamical systems with fractional derivative term under wide-band excitation, Math. Probl. Eng. (2016) 9.

[18] Y. Xu, Y. Li, D. Liu, Response of fractional oscillators with viscoelastic term under random excitation, J. Comput. Nonlinear Dyn. 9 (3) (2014) 31015–31018.

[19] L.C. Chen, Q.Q. Zhuang, W.Q. Zhu, Response of SDOF nonlinear oscillators with lightly fractional derivative damping under real noise excitations, Eur. Phys. J. Special Top. 193 (1) (2011) 81–92.

[20] Y. Kun, L. Li, T. Jiaxiang, Stochastic seismic response of structures with added viscoelastic dampers modeled by fractional derivative, Earthq. Eng. Eng. Vib. 2 (1) (2003) 133–139.

[21] P.D. Spanos, G.I. Evangelatos, Response of a non-linear system with restoring forces governed by fractional derivatives: Time domain simulation and statistical linearization solution, Soil Dyn. Earthq. Eng. 30 (9) (2010) 811–821.

[22] N. Colinas-Armijo, M. Di Paola, Step-by-step integration for fractional operators, Commun. Nonlinear Sci. Numer. Simul. 59 (2018) 292–305.

[23] G. Jumarie, Path integral for the probability of the trajectories generated by fractional dynamics subject to Gaussian white noise, Appl. Math. Lett. 20 (8) (2007) 846–852.

[24] I.A. Kougioumtzoglou, A. Di Matteo, P.D. Spanos, A. Pirrotta, M. Di Paola, An efficient Wiener path integral technique formulation for stochastic response determination of nonlinear MDOF systems, J. Appl. Mech. 82 (10) (2015) 101005–101007.

[25] A. Lotfi, S.A. Yousefi, A numerical technique for solving a class of fractional variational problems, J. Comput. Appl. Math. 237 (1) (2013) 633–643.

[26] A. Di Matteo, I.A. Kougioumtzoglou, A. Pirrotta, P.D. Spanos, M. Di Paola, Stochastic response determination of nonlinear oscillators with fractional derivatives elements via the Wiener path integral, Probab. Eng. Mech. 38 (2014) 127–135.

[27] I.A. Kougioumtzoglou, P.D. Spanos, Harmonic wavelets based response evolutionary power spectrum determination of linear and non-linear oscillators with fractional derivative elements, Int. J. Non-Linear Mech. 80 (2016) 66–75 Dynamics, Stability, and Control of Flexible Structures.

[28] G. Failla, Stationary response of beams and frames with fractional dampers through exact frequency response functions, J. Eng. Mech. 143 (5) (2017) D4016004.

[29] G. Alotta, G. Failla, M. Zingales, Finite-element formulation of a nonlocal hereditary fractional-order Timoshenko beam, J. Eng. Mech. 143 (5) (2017) D4015001.

[30] M. Di Paola, A. Pirrotta, F.P. Pinnola, S. Di Lorenzo, Stochastic response of fractionally damped beams, Probabilistic Eng. Mech. 35 (2014) 37–43.

[31] M. Enelund, B. Lennart Josefson, Time-domain finite element analysis of viscoelastic structures with fractional derivatives constitutive relations, AIAA J. 35 (10) (1997) 1630–1637.

[32] G. Cottone, M. Di Paola, Fractional spectral moments for digital simulation of multivariate wind velocity fields, J. Wind Eng. Ind. Aerodyn. 99 (6) (2011) 741–747 The Eleventh Italian National Conference on Wind Engineering, IN-VENTO-2010, Spoleto, Italy, June 30th - July 3rd 2010.

[33] V. Denoël, Multiple timescale spectral analysis, Probab. Eng. Mech. 39 (2015) 69–86.

[34] V. Denoël, On the background and biresonant components of the random response of single degree-of-freedom systems under non-Gaussian random loading, Eng. Struct. 33 (8) (2011) 2271–2283.

[35] T. Canor, L. Caracoglia, V. Denoël, Perturbation methods in evolutionary spectral analysis for linear dynamics and equivalent statistical linearization, Probab. Eng. Mech. 46 (2016) 1–17.

[36] V. Denoël, L. Carassale, Response of an oscillator to a random quadratic velocity-feedback loading, J. Wind Eng. Ind. Aerodyn. 147 (2015) 330–344.

[37] V. Denoël, Estimation of modal correlation coefficients from background and resonant responses, Struct. Eng. Mech.: Int. J. 32 (6) (2009) 725–740.

[38] T. Canor, N. Blaise, V. Denoël, Efficient uncoupled stochastic analysis with non-proportional damping, J. Sound Vib. 331 (24) (2012) 5283–5291.

[39] G. Solari, G. Piccardo, Probabilistic 3-D turbulence modeling for gust buffeting of structures, Probab. Eng. Mech. 16 (1) (2001) 73–86.
[40] E. Simiu, R. Scanlan, Wind Effects On Structures, third ed., John Wiley and Sons, New-York, 1996.
[41] V. Valimaki, T.I. Laakso, Principles of fractional delay filters, in: 2000 IEEE International Conference on Acoustics, Speech, and Signal Processing. Proceedings (Cat. No.00CH37100), vol. 6, 2000, pp. 3870–3873.
[42] E.J. Hinch, Perturbation Methods, vol. 1, Cambridge University Press, Cambridge, 1991, p. 160.
[43] A. Preumont, Random Vibration and Spectral Analysis, Kluwer Academic Publishers, 1994, p. 288.
[44] L. Chen, Q. Zhuang, W. Zhu, First passage failure of MDOF quasi-integrable Hamiltonian systems with fractional derivative damping, Acta Mech. 222 (3) (2011) 245–260.
[45] H. Vanvinckenroye, V. Denoël, Average first-passage time of a quasi-Hamiltonian Mathieu oscillator with parametric and forcing excitations, J. Sound Vib. 406 (2017) 328–345.
[46] Wolfram Research, Inc. Mathematica, Version 11.0, Champaign, IL, 2016.